



Blastability evaluation for rock mass fragmentation in Iran central iron ore mines



Akbari Majid ^{a,*}, Lashkaripour Gholamreza ^a, Yarahamdi Bafghi Alireza ^b, Ghafoori Mohammad ^a

^a Department of Geology, Ferdowsi University of Mashhad, Mashhad 91779-48974, Iran

^b Department of Mining Engineering, Yazd University, Yazd 89195-741, Iran

ARTICLE INFO

Article history:

Received 29 March 2014

Received in revised form 25 May 2014

Accepted 26 July 2014

Available online 7 February 2015

Keywords:

Rock mass

Blast fragmentation

Blasting

Size distribution

Connector

ABSTRACT

In this research, we investigated the influence of rock mass properties, blast design parameters and explosive properties on blast fragmentation. Rock mass properties were evaluated in 51 blasting blocks using engineering geological mapping of 1961 meters of the scanline, experiments on intact rock samples and measuring P-wave velocity (V_p) for 1771 meters of seismic profiles. The results indicate that increasing spacing, persistence, opening, roughness, waviness of discontinuities, and V_p and uniaxial compressive strength (UCS) of intact rock as well as the increase of discontinuities angle with the bench face of blasting block will increase the size distribution of blasted rocks. In addition, evaluation of the influence of connector type, specific drilling and specific charge has shown that using the Nonel system will decrease the mean size of fragmentation. It is also demonstrated that increasing specific drilling and specific charge quantities will result in the increase of mean size of fragmentation.

© 2015 Published by Elsevier B.V. on behalf of China University of Mining & Technology.

1. Introduction

Blasting is one of the main operations in opencast mining. Blasting operation is influenced by various factors that can be classified into three categories: rock mass properties, blast design parameters and explosive properties. Burden, spacing between drillholes, stem height, drillhole inclination, diameter and length, drilling pattern, blasting direction, subdrilling and blasting sequence are blast design parameters that are controllable. Explosive materials parameters include explosive type, density, strength, resistance to moisture and heat, and specific charge, all of which are also controllable. The third group consists of the parameters related to the nature of the rock mass. These uncontrollable parameters are among the most important influencing variables in the blasting results [1–5].

When two different rock masses are subjected to identical blast geometry and energy input from explosives, they will produce quite different degrees of fragmentation. This is because the rock masses have inherently different resistance to fragmentation by blasting which is referred to as the blastability of a rock mass [3].

Parameters related to the nature of rock mass consist of physical and mechanical properties of intact rock and discontinuities. Intact rock properties include strength, hardness, elasticity, deformability, density, etc. They are dependent on rock texture, internal

bonds, and composition and distribution of rock forming minerals. Discontinuity properties include orientation, spacing, persistence, opening, roughness, waviness and infilling materials created by a range of long-term geological processes. There are several different researches on the influence of rock mass and intact rock properties on blasting operations, all of which clearly indicate that the properties of blasted rock mass has a significant impact on blasting results [3,4] and [6–12].

The aim of this research is to evaluate and measure all influential parameters in blast fragmentation. For this purpose, 51 blasting blocks were selected and their rock mass properties were evaluated by measuring the characteristics of discontinuities in 1961 meters of scanline, experimenting upon intact rock samples and measuring P-wave velocity (V_p) in 1771 meters of seismic profiles in Choghart, Chadormalu and Sechahun mines. Finally, the influence of mentioned parameters on blast fragmentation was investigated.

2. Geology of study areas

The studied areas consist of Choghart, Chadormalu and Sechahun iron ore mines. These mines are located in Bafgh block in ferrous zone of Anarak–Bafgh–Kerman. The geographical location of the study area is shown in Fig. 1.

From the geological point of view, Choghart ore deposit is located in Precambrian formations of central Iran (Morad series).

* Corresponding author. Tel.: +98 9155169396.

E-mail address: ma_ak772@stu-mail.um.ac.ir (M. Akbari).

This series had undergone different changes such as metamorphism and metasomatism. The enclosing rocks of this ore deposit are mainly granite, quartz albitophyre and metasomatites. From the tectonic point of view, in Choghart ore deposit, three main categories of structural factors and faulting can indicate the effect of significant Panafrican, Cimmerian and Alpine events. The Panafrican structures are considered as the main factors of ore concentration and regional changes. These structures are deep faults with N–S and E–W strikes.

Sechahun ore rocks consist of Morad series rocks. In Sechahun ore deposit domain, intrusive rocks are mainly composed of diorite, granite, granophyre and syenite. In addition, the different combinations of dikes are approximately E–W strikes and high dips of 75–80°. Chadormalu ore deposit consists of two north and south anomalies. Due to metasomatic and magmatic conditions and high tectonic activities, this ore deposit has a complex geological condition. Discontinuities in ore deposits mostly have NW–SE strikes and 70–80°NW dip angles. Mineral mass was fractured by granitic and dioritic-dikes which have 15–45° dip angle and 1–20 meters thickness. In Cambrian period, ore deposit domain consists of granite gneiss, biotite gneiss and part of amphibolite facies. Ore deposit rocks included crystalline schist, fine grain schist, quartzite schist, biotite schist, quartzite, amphibolite and marbles. In Upper Cambrian period it is consisted of volcanic rocks, dolomites and sandstones.

3. Extraction operations in the studied mines

Extraction operation of iron ore in the studied mines are done by opencast mining. Extraction stages include drilling operations, blasting, loading and hauling [13]. Hole drilling is done by rotary and percussion machinery in different diameter (165, 200 and 251 mm). In these mines, blast holes are controlled in ANFO (in dry conditions) and Emulite (for aqueous conditions) as the main explosive, and the detonating cord and Nonel system are applied for initiation. Some related characteristics of extraction in the studied mines are presented in Table 1 [14].

4. Rock mass properties

Rock mass is composed of two parts of intact rock and discontinuities. Discontinuities include structures in rock mass such as

Table 1
Characteristics of study mines.

Mine	Mineable ore reserve (million ton)	Bench height (m)	Bench width (m)	Bench Face Angle (°)	Overall Angle of Pit wall (°)
Choghart	177.2	10–12.5	8–10	70	38–50
Chadormalu	320	15	10	69.5	50–55
Sechahun	132	10	10	69.5	55

joints, faults, fractures, bedding and other weakness surfaces that significantly influence the engineering and mechanical properties of rock mass [15]. The presence of one or several sets of discontinuities in a rock mass under loading and unloading leads to anisotropy. Also, in contrast to intact rocks, jointed rocks have higher permeability, less shear strength along discontinuity planes, and higher deformability and lower tensile strength in perpendicular direction of their plane. Furthermore, discontinuities lead to scale effects and the resulting intersection blocks can lead to instability problems. Therefore, in engineering studies of rock masses, both engineering properties of intact rock and discontinuities have to be considered.

4.1. Measuring of rock mass properties

Line mapping method was used to measure engineering geology properties of rock mass in rock outcrops. In this method, desirable engineering properties are surveyed along the scanline on the rock outcrop. In line mapping, the length of scanline was variable from 10–100 meters. Priest and Hudson suggested that the length of scanline must be at least fifty times than that of the average spacing of discontinuities [16]. However, the International Society of Rock Mechanic has advised that the length of a scanline should normally be 50–100 meters [15] and [17]. In this method, we can choose the length of scanline based on the major changes of rock mass properties such as lithological changes, structural changes or even presence of a fault or fault zone or numerous changes in the weathering rate of rock mass. By considering these changes, we can use a new scanline for surveying rock mass properties.

In this study, discontinuities properties of 51 blasting blocks were measured in a length of 1961 meters of the scanline. Along these scanlines, properties of 7176 discontinuities were evaluated.

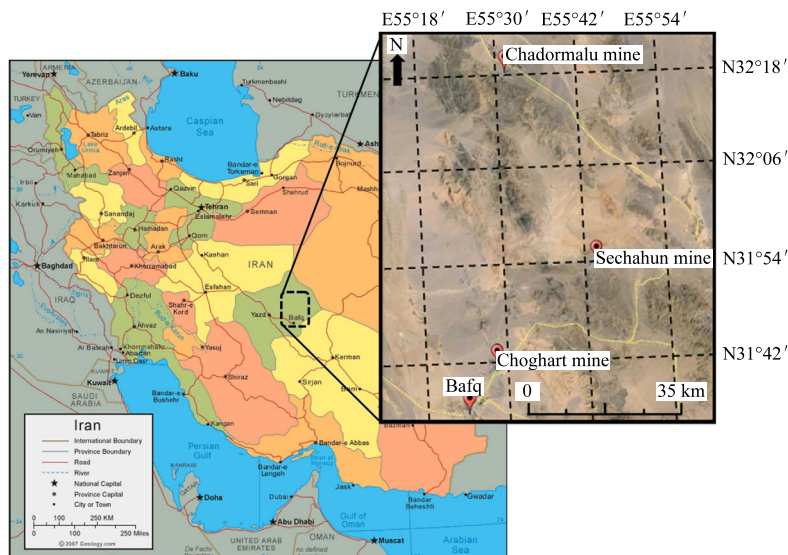


Fig. 1. Geographical location of study areas.

Table 2
Average orientation of discontinuities in studied mines.

Mine	Dip (°)	Dip direction (°)
Choghart	61.5	183.0
Chadormalu	63.8	174.7
Sechahun	59.0	169.0

Most of the surveys were from Choghart mine with surveys of 3838 discontinuities along 1062.5 meters of the scanline. After that, 2125 discontinuities were surveyed along 565 meters of scanline in Chadormalu mine. Lastly, 1213 discontinuities were surveyed along 334 meters of scanline in Sechahun mine. Statistical analysis of dip, dip direction and spacing data in the studied mines indicates that the distribution of dip and dip direction data is normal and distribution of spacing data is exponential (Figs. 2–4, Table 2).

Statistical study of other discontinuities properties showed that 95.6% of discontinuities are of joint type in Choghart mine. 46% of discontinuities had low persistence (1–3 m), 58.9% had open openings (0.5–2.5 mm), 60.6% had clay infilling and 50.3% had moderate spacing (20–60 cm). Furthermore, 84.1% of these discontinuities

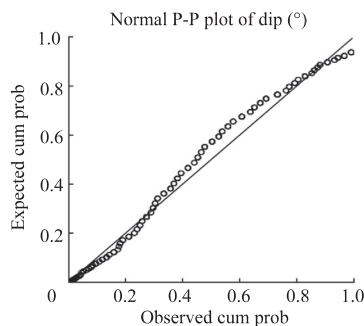


Fig. 2. P-P plots of dip of Choghart mine.

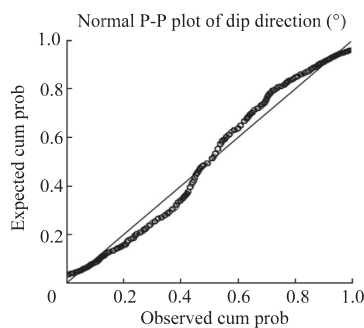


Fig. 3. P-P plots of dip direction of Choghart mine.

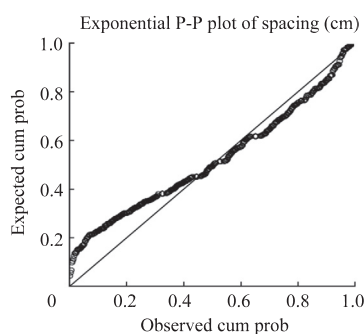


Fig. 4. P-P plots of spacing of Choghart mine.

Table 3
Descriptive statistic results of measured parameters in intact rock.

Statistic	UCS (MPa)	UTS (MPa)	Vp (m/s)	Density ($\times 10^3$ kg/m ³)
Mean	58.5	6.47	5273.0	2.77
Maximum	110.5	12.15	6166.7	3.42
Minimum	15.23	1.74	4023.4	2.55
Standard deviation	23.4	2.71	494.8	0.24

had undulating surface and 60.2% of them had a smooth surface. In Chadormalu mine, 96.5% of the prominent type of discontinuities were related to joints. 60.4% of the discontinuities had low persistence, 47.2% had open openings, 61.4% had clay infilling and 52% had moderate spacing. Surface of 52.5% of discontinuities were planar and 49% of them had a smooth surface. In Sechahun mine 91.3% of discontinuities were of joint type. 56% of openings had low persistence, 55.8% had open opening, 73.7% had clay infilling and 72.8% had moderate spacing. Most of the discontinuities had 93.8% of undulating surface and 75.3% of smooth surface.

To measure intact rock properties, derived cores of rock samples of blasting blocks with no plane of weakness were studied in the laboratory and parameters such as uniaxial tensile strength (UTS), uniaxial compressive strength (UCS) and density of the samples were measured. Vp in rock samples were also determined using Ultrasonic Pulse Velocity instrument (PUNDIT 6). The descriptive statistical results are presented in Table 3.

4.2. Measurement of seismic properties of rock mass

In this research, seismic refraction method was used to obtain seismic wave velocity in the rock mass. Equipment used for seismic data acquisition included the source for creating seismic waves, geophones, battery, connector cables and recorder. Seismic waves were created by the energy applied to the ground. In field seismic surveys, seismic waves can be created manually by heavy machinery or explosive materials. In this study, a sledge (approximately 18 kg weight) was used to create the seismic source.

Geophones used in the survey were electromagnetic PE-3 geophones made by a Dutch sensor company with a normal frequency of 10 Hz and the seismograph was TERRALOC Mk8 made by the Swedish ABEM company. This seismograph has twelve channels and is appropriate for cost-effective refraction and high-resolution reflection surveys, tomography and vibration measurements in all weather conditions. It has an internal storage of 80 GB and frequency range of 2–4000 Hz. SeisTw software installed on the seismograph was used for primary survey and observation of recorded data in the field. For final processing of data and calculation, the Vp, Reflex-Win 5.0.5 software was used.

Based on the length and conditions of blasting blocks, appropriate arrangement of two geophones, 3 or 5 meters spacing were used. Seven shotpoints were used in the whole survey in the length of the profile from which five shotpoints were through the profile and four of shotpoints were out of it. Fig. 5 demonstrates the longitudinal wave in the survey process.

Seismic properties of rock mass were surveyed along 71 seismic profiles. Based on different spacing between geophones, the length of all surveyed profiles is 1771 meters (see Table 4).

5. Determination of size distribution of blasted rocks

To determine the size distribution of blasted rocks, the method of digital image processing was done by using Split-Desktop software. This image processing software was first developed by Arizona University and works with gray scale images of

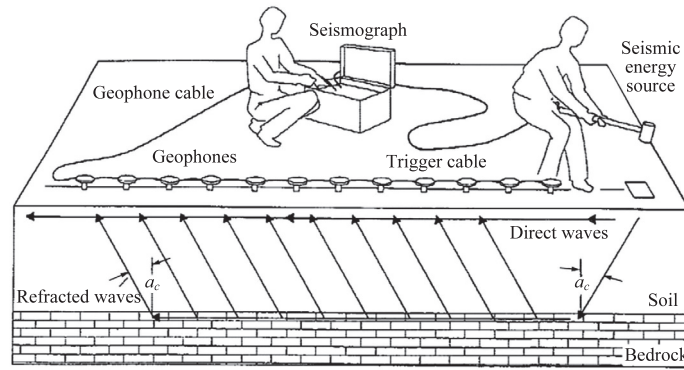


Fig. 5. A twelve-channel seismograph showing the path of direct and refracted seismic waves in a two-layer soil/rock system [18].

Table 4
Seismic refraction results in the study area.

Mine	Profile No.	Profiles length (m)	Mean Vp (m/s)	Standard deviation	Maximum Vp (m/s)	Minimum Vp (m/s)
Choghart	36	869	1265	180.2	1652.0	967.3
Chadormalu	27	682	1343	304.5	2146.8	868.2
Sechahun	8	220	2134	360.3	2919.2	1668.3

Table 5
Descriptive statistics results from calculation of percent passing sizes in studied blasted blocks.

Statistics	P30 (mm)	P50 (mm)	P80 (mm)	Top size (mm)
No. of samples	51.0	51.0	51.0	51.0
Mean	56.5	128.4	308.1	706.8
Standard deviation	36.4	69.8	142.2	233.6
Minimum	9.4	35.5	116.2	269.6
Maximum	237.0	268.3	753.6	1342.9

fragmented rocks (Split Engineering). These images can be acquired from muck piles, haul trucks, waste dumps, stockpiles and conveyor belts [19]. The main steps involved in the Split software include acquiring digital images (either automatically or manually), preprocessing the images to correct for illumination problems and omitting unacceptable images accordingly, scaling images, delineating individual fragments in each image, editing of the delineated fragments to ensure high quality of results, processing multiple images to get an average distribution, and plotting or exporting the results of size distribution [20]. All the images were taken by a digital camera with 10 megapixel resolution in an average scale. In this scale, the horizontal length of images must be approximately 3 meters.

The angle of the slope relative to the axis of the camera lens is an important factor in acquiring images of muck piles. If it is not perpendicular, apparent scale of the image varies continuously from the bottom to the top of the slope. There are several ways to correct the scale in muck pile images [21]. The simplest way is to place two objects of known size in the image, one is on the bottom of the slope and the other is on the top of the slope. To get this point in this study, two balls with specific diameters were used. After deleting undesirable images, approximately a total of 1500 images and an average of 29 images for each blasted block were processed. Statistical properties of size distribution of blasted rocks for all 51 studied blasted blocks are presented in Table 5.

6. Effect of rock mass properties on fragmentation

To find all effective parameters on blasting results, rock mass properties, blasting design parameters and explosive properties

for all blasted blocks were studied. To study rock mass properties, these features were measured along 1961 meters of scanline and 1771 meters of seismic profiles. Then the effect of these properties on blasting fragmentation of the same rock mass was studied for percent passing sizes P30, P50 and P80. As depicted in Figs. 6–12, the investigation results confirmed the relation between rock mass properties and obtained fragmentation so that with increase of discontinuities spacing in the rock mass, blasted rocks sizes increase as well (Fig. 6). In addition, as discontinuities persistence in rock mass increases, the size of blasted rocks increase too (Fig. 7).

Studying the effects of discontinuities openings on blasting fragmentation of rock mass also indicates an increasing trend of size distribution of blasted rocks with the increased discontinuities opening of the rock mass (Fig. 8). Similarly, effects of discontinuity surface's evaluate condition confirmed that by increasing roughness and waviness of this surface, size distribution of blasted rocks increase as well (Figs. 9 and 10). To investigate the effects of discontinuity orientation on obtaining fragmentation, acute angles

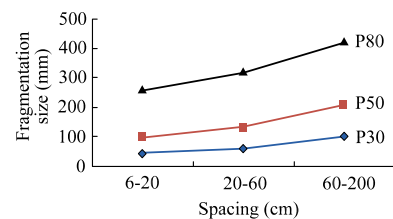


Fig. 6. Effect of discontinuities spacing on fragmentation.

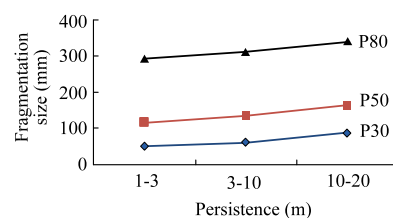


Fig. 7. Effect of discontinuities persistence on fragmentation.

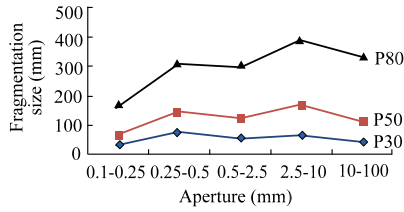


Fig. 8. Effect of discontinuities opening on fragmentation.

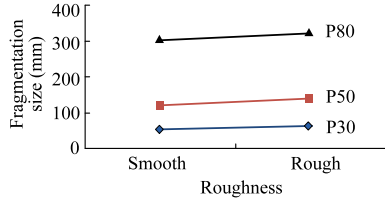


Fig. 9. Effect of roughness of discontinuity surface on fragmentation.

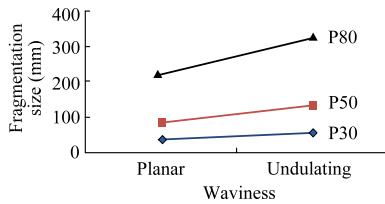


Fig. 10. Effect of waviness of discontinuity surface on fragmentation.

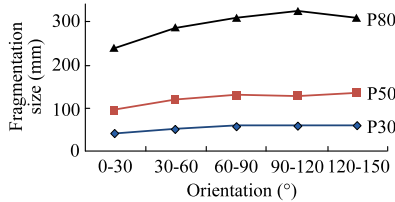


Fig. 11. Effect of discontinuities orientation on fragmentation.

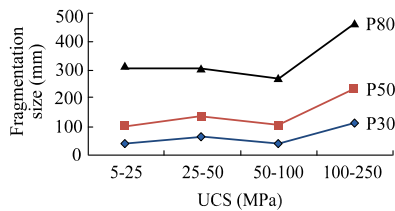


Fig. 12. Effect of uniaxial compressive strength on fragmentation.

between dip direction of each major discontinuity set and the bench face of each blasted block were calculated. The obtained angles and blasting fragmentation were studied for each blasting block. Results demonstrated that when angles are close to 90°, discontinuities are perpendicular to bench face, the size of blasted rocks increases (Fig. 11). UCS of intact rock is another effective parameter in blasting results so that by increasing UCS of intact rock, the size of blasted rocks increases and more energy should be applied to the rock for more fragmentation (Fig. 12).

To investigate the relations between rock mass properties and obtained fragmentation, different models were fitted to the data. The best fitted model between each rock mass property and percent passing sizes P30, P50 and P80, and their determination coefficients (R^2) are presented in Table 6. To assess the influence of blasting fragmentation on downstream mining processes, different linear regression models were fitted on rock mass properties and fragmentation data. Lastly, the best linear relation was found between rock mass properties and percent passing size P80 with determination coefficient of 0.927, as shown in Eq. (1).

$$P80 = -9.187x_1 + 7.031x_2 + 117.327x_3 + 3.894x_4 - 0.665x_5 - 382.847x_6 + 0.979x_7 \quad (1)$$

where x_1 is the discontinuity persistence, m; x_2 the discontinuity opening, mm; x_3 the discontinuity spacing, m; x_4 the RQD (Rock Quality Designation); x_5 the UCS of intact rock, MPa; x_6 the velocity index of seismic waves; and x_7 the orientation effect, degree, respectively.

7. Effects of blasting design parameters and explosive properties on fragmentation

To study the effects of blasting design parameters, effects of specific drilling and blasting system types on the size of blasted rocks were investigated. Specific charge parameter was used to evaluate the effects of explosive properties on final fragmentation. Explosives such as ANFO, Emulite and Azar powder were used in blasting blocks. Due to the widespread use of ANFO explosives, equivalent weight for each explosive was calculated when using the energy of each explosive. Then the specific charge for each blasting block was calculated based on the ANFO explosive (see Table 7).

Two blasting systems are used in the studied mines. The main difference of these blasting systems is the type of connector. The connector is used in one system detonating cord and the other Nonel system. In the detonating cord, detonation starts from the top of the hole and detonation delay occurs on the surface. However, in Nonel, explosion starts from the bottom of the hole and delay is placed in detonators with higher accuracy. These two differences lead to different results in the size distribution of blasted rocks and geometric shape of blasting blocks (surface after explosion). Based on the mentioned advantages, the application of Nonel is increasing.

Table 6
The best fitting model between rock mass properties and fragmentation.

X	Y = P30		Y = P50		Y = P80	
Discontinuity persistence (m)	$y = x^{2.34}$	$R^2 = 0.901$	$y = x^{2.843}$	$R^2 = 0.9$	$y = x^{3.371}$	$R^2 = 0.896$
Discontinuity opening (mm)	$y = e^{(4.008/x)}$	$R^2 = 0.652$	$y = e^{(4.901/x)}$	$R^2 = 0.66$	$y = e^{(5.854/x)}$	$R^2 = 0.666$
Discontinuity spacing (m)	$y = x^{-2.297}$	$R^2 = 0.717$	$y = x^{-2.847}$	$R^2 = 0.745$	$y = x^{-3.428}$	$R^2 = 0.764$
Rock Quality Designation	$y = e^{1.043x}$	$R^2 = 0.981$	$y = x^{1.047}$	$R^2 = 0.989$	$y = x^{1.247}$	$R^2 = 0.994$
UCS of intact rock (MPa)	$y = x^{0.964}$	$R^2 = 0.973$	$y = x^{1.176}$	$R^2 = 0.98$	$y = x^{1.4}$	$R^2 = 0.983$
Vp of intact rock (m/s)	$y = x^{0.451}$	$R^2 = 0.977$	$y = x^{0.552}$	$R^2 = 0.989$	$y = x^{0.658}$	$R^2 = 0.994$
Vp of Rock mass (m/s)	$y = x^{0.532}$	$R^2 = 0.975$	$y = x^{0.651}$	$R^2 = 0.985$	$y = x^{0.776}$	$R^2 = 0.993$
Velocity index	$y = x^{-2.812}$	$R^2 = 0.938$	$y = x^{-3.439}$	$R^2 = 0.95$	$y = x^{-4.096}$	$R^2 = 0.953$
Orientation effect (degree)	$y = x^{0.902}$	$R^2 = 0.962$	$y = x^{1.013}$	$R^2 = 0.974$	$y = x^{1.315}$	$R^2 = 0.98$

Among the studied blocks, 16 blocks were blasted by detonating cord method and 35 blocks by Nonel. Influences of application of each blasting method on fragmentation were evaluated. As shown in Fig. 13, by applying Nonel system in blasting operations, the minimum values of percent passing sizes P50 and P80 and the top size were reduced.

On the other hand, Nonel system applications increased the maximum amount of percent passing sizes P30 and reduced the maximum amount of percent passing sizes P80 and the top size (Fig. 14). In general, applying Nonel system in blasting operations leads to reducing mean value in all percent passing sizes in studied mines (Fig. 15).

Moreover, influence of blasting system on specific charge was investigated for the same fragmentation intervals. As demonstrated in Figs. 16–19, applying Nonel system reduces the specific charge for different percent passing sizes in the same fragmentation intervals. These results confirm that to achieve desirable fragmentation, Nonel system requires less explosive materials compared with detonating cord system.

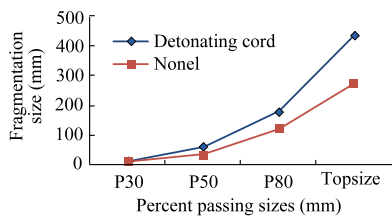


Fig. 13. Effect of blasting system type on minimum values of fragmentation size.

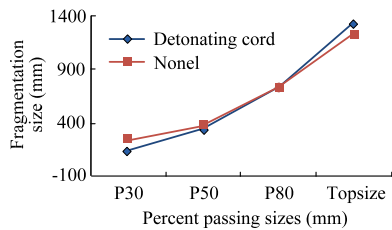


Fig. 14. Effect of blasting system type on maximum values of fragmentation size.

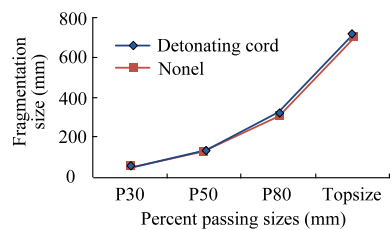


Fig. 15. Effect of blasting system type on mean values of fragmentation size.

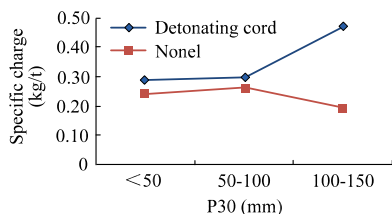


Fig. 16. Effect of blasting system type on specific charge for percent passing sizes P30.

The research done on the effects of specific drilling on size distribution of blasted rocks showed that by increasing specific drilling, the mean size of blasted rocks increases as well (Fig. 20). Results also indicate that by increasing the amount of specific charge (kg/ton) to 0.2–0.3, the mean size of fragmented rocks

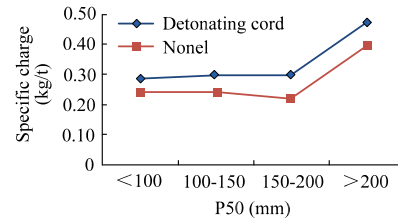


Fig. 17. Effect of blasting system type on specific charge for percent passing sizes P50.

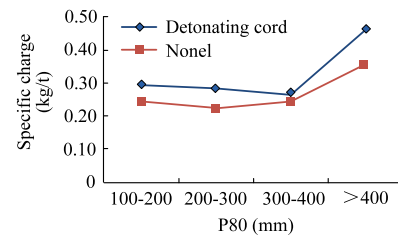


Fig. 18. Effect of blasting system type on specific charge for percent passing sizes P80.

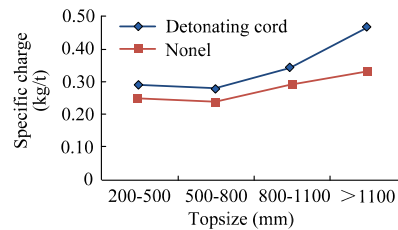


Fig. 19. Effect of blasting system type on specific charge for top size.

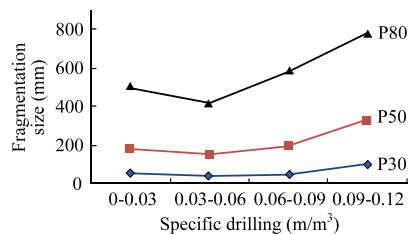


Fig. 20. The specific drilling effect on fragmentation.

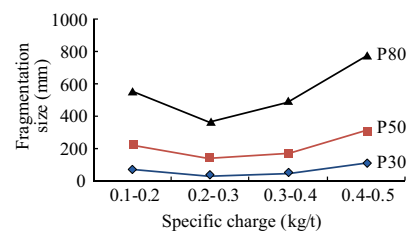


Fig. 21. The specific charge effect on fragmentation.

Table 7

Descriptive statistic results of blasting design parameters and explosive properties in the studied blasting blocks.

Statistic	Specific charge (kg/ton)	Specific charge (kg/m ³)	Specific drilling (m/m ³)	Spacing (m)	Burden (m)
Mean	0.27	0.77	0.052	5.07	5.04
Standard deviation	0.099	0.34	0.027	1.75	1.23
Minimum	0.11	0.31	0.02	3.0	3.0
Maximum	0.48	1.64	0.11	8.50	7.50

Table 8

The fitted best model between blasting design parameters and explosive properties with fragmentation.

X	Y = P30		Y = P50		Y = P80	
Spacing (m)	$y = x^{2.34}$	$R^2 = 0.92$	$y = x^{2.867}$	$R^2 = 0.93$	$y = x^{3.43}$	$R^2 = 0.95$
Burden (m)	$y = e^{(17.66/x)}$	$R^2 = 0.95$	$y = x^{2.892}$	$R^2 = 0.96$	$y = x^{3.46}$	$R^2 = 0.97$
Specific drilling (m/m ³)	$y = x^{-1.205}$	$R^2 = 0.94$	$y = x^{-1.476}$	$R^2 = 0.95$	$y = x^{-1.765}$	$R^2 = 0.96$
Specific charge (kg/m ³)	$y = e^{(2.257/x)}$	$R^2 = 0.86$	$y = e^{(2.76/x)}$	$R^2 = 0.87$	$y = e^{(3.297/x)}$	$R^2 = 0.88$
Specific charge (kg/ton)	$y = x^{-2.645}$	$R^2 = 0.9$	$y = x^{-3.238}$	$R^2 = 0.92$	$y = x^{-3.868}$	$R^2 = 0.93$

reduces and after that with specific charge increasing, the mean size of fragmented rocks increases too (Fig. 21).

To quantitatively analyze the relation between the amount of P30, P50 and P80, blasting design parameters and explosive properties, different models were fitted to data. Table 8 contains the best fitted model with their determination coefficient.

Additionally, with linear regression, different linear models were fitted to data for all parameters affecting fragmentation and percentile amounts of the passing sizes. Finally, the best linear relation between these parameters and the amount of P30, P50 and P80 were obtained, as shown in Eqs. (2)–(4).

$$P30 = -1.987x_1 + 1.415x_2 + 26.546x_3 + 0.031x_4 - 65.152x_5 + 0.21x_6 + 0.375x_7 - 33.184x_8 + 523.91x_9 (R^2 = 0.804) \quad (2)$$

$$P50 = -5.155x_1 + 3.357x_2 + 49.53x_3 - 0.124x_4 - 141.839x_5 + 0.435x_6 + 0.992x_7 + 2.438x_8 + 905.52x_9 (R^2 = 0.853) \quad (3)$$

$$P80 = -9.822x_1 + 6.25x_2 + 107.894x_3 - 0.689x_4 - 375.7x_5 + 0.998x_6 + 2.615x_7 + 640.45x_8 - 921.65x_9 (R^2 = 0.874) \quad (4)$$

where x_1 is the discontinuity persistence, m; x_2 the discontinuity opening, mm; x_3 the discontinuity spacing, m; x_4 the UCS of intact rock, MPa; x_5 the velocity index of seismic waves; x_6 the orientation effect, degree; x_7 the RQD (Rock Quality Designation); x_8 the specific charge, kg/ton; and x_9 the specific drilling, m/m³, respectively.

8. Conclusions

Based on the importance of optimization in blast fragmentation in mining activities, this paper tried to study all effective parameters on blast fragmentation. For this purpose, rock mass properties, blasting design parameters and explosive properties were evaluated in 51 blasting blocks. Results of statistical analysis indicate that in Choghart, Chadormalu and Sechahun mines, the mean dip angles of discontinuities are 61.5°, 63.8°, 59° and mean dip directions are 183°, 174.8° and 169°, respectively. Mainly in all mines, discontinuities have low persistence (1–3 m), open opening (0.5–2.5 mm), clay infilling and moderate spacing (20–60 cm). In Choghart and Sechahun mines, discontinuities mainly have undulating and smooth surface while in Chadormalu, mine discontinuities mainly have planar and smooth surface. By analyzing the intact rock samples taken from each blasting blocks in the studied mines, average UCS, Brazilian tensile strength, V_p and density are calculated as 58.5 MPa, 6.47 MPa, 5273 m/s and 2.77 ton/m³,

respectively. Implementing the seismic refraction in the studied area indicates that mean V_p is 1265 m/s in Choghart mine, 1342.9 m/s in Chadormalu mine and 2134 m/s in Sechahun mine. Furthermore, to measure the blast fragmentation, digital image processing methods are used. For this purpose, after processing 1500 images taken from muck piles surface, the average amount of P30, P50, P80 and top size are obtained as 56.5 mm, 128.4 mm, 308.1 mm and 706.8 mm, respectively. Studying of the fragmentation changes based on rock mass property changes shows that, by increasing the spacing, persistence and opening of discontinuities, roughness and waviness of discontinuity surface, UCS and V_p of intact rock, as well as the increase of the perpendicular state of discontinuities to bench face of blasting blocks, the size of blasted rocks increases. In addition, evaluation of the influence of connector type shows that applying Nonel system in blasting operations will reduce all percent passing sizes of blasted rocks. The results represent that for achieving desirable blasting fragmentation, Nonel system requires less explosive materials compared with detonating cord system. The mean specific drilling in blasting blocks is 0.052 m/m³ and the average specific charge is 0.27 kg/ton. Finally, evaluation of influence of specific drilling and specific charge on size distribution of blasted rocks indicates that the mean size of blasted rocks will increase by increasing specific drilling and specific charge.

References

- [1] Konya CJ, Walter EJ. Rock blasting and overbreak control. US: Federal Highway Administration, No. FHWA-HI-92-001; 1991.
- [2] Bhandari S. Engineering rock blasting operations. Rotterdam, Brookfield: A. A. Balkema; 1997.
- [3] Latham JP, Lu P. Development of an assessment system for the blastability of rock masses. Int J Rock Mech Min Sci 1999;36:41–55.
- [4] Azimi Y, Osanloo M, Aakbarpour-Shirazi M, Aghajani BA. Prediction of the blastability designation of rock masses using fuzzy sets. Int J Rock Mech Min Sci 2010;47(7):1126–40.
- [5] Kulatilake PHSW, Hudaverdi T, Wu Q. New prediction models for mean particle size in rock blast fragmentation. Geotech Geol Eng 2012;30:665–84.
- [6] Hagan TN. The effect of rock properties on the design and results of tunnel blasts. J Rock Mech Tunneling Technol 1995;1(1):25–39.
- [7] Aler J, Du Mouza J, Arnould M. Measurement of the fragmentation efficiency of rock mass blasting and its mining applications. Int J Rock Mech Min Sci Geomech Abstr 1996;33(2):125–39.
- [8] Han J, Wei YX, Shou YX. Artificial neural network method of rock mass blastability classification. In: Proceedings of the fifth international conference on geo computation. London; 2000. p. 23–25.
- [9] Thornton D, Kanchibolita SS, Brunton I. Modelling the impact and blast design variation on blast fragmentation. Int J Blasting Fragmentation 2002;6(2):171–2.
- [10] Kacar G, Ozgenoglu A, Bilgin HA. Effect of discontinuity orientation and spacing on the blasting performance in some open cast mines of TKI-Turkey.

- In: ISRM 2003-technology roadmap for rock mechanics. Johannesburg; 2003. p. 595–601.
- [11] Kaushik D, Phalguni S. Concept of blastability – an update. *Indian Mining Eng J* 2003;42(8&9):24–31.
- [12] Kilic AM, Yasar E, Erdogan Y, Ranjith PG. Influence of rock mass properties on blasting efficiency. *Sci Res Essay* 2009;4(11):1213–24.
- [13] Karamia A, Afuni-Zadehb S. Sizing of rock fragmentation modeling due to bench blasting using adaptive neuro-fuzzy inference system (ANFIS). *Int J Min Sci Technol* 2013;23(6):809–13.
- [14] Daya AA. Reserve estimation of central part of Choghart north anomaly iron ore deposit through ordinary kriging method. *Int J Min Sci Technol* 2012;22(4):573–7.
- [15] ISRM (International Society for Rock Mechanics). Commission on standardization of laboratory and field tests, Suggested methods for the quantitative description of discontinuities in rock masses. *Int J Rock Mech Min Sci Geomech Abstr* 1978;15(6):319–68.
- [16] Wines DR, Lilly PA. Measurement and analysis of rock mass discontinuity spacing and frequency in part of the Fimiston open pit operation in Kalgoorlie, Western Australia: a case study. In *J Rock Mech Min Sci* 2002;39:589–602.
- [17] Wyllie DC, Mah CW. *Rock slope engineering: civil and mining*. 4th ed. New York: Taylor & Francis e-Library, Spon Press; 2005.
- [18] ISRM (International Society for Rock Mechanics). Standard guide for using the seismic refraction method for subsurface investigation. ASTM D 5777–00; 2000:14.
- [19] Sanchidrian JA, Segarra P, Lopez LM. A practical procedure for the measurement of fragmentation by blasting by image analysis. *J Rock Mech Rock Eng* 2006;39(4):359–82.
- [20] Kemeny J, Mofya E, Kaunda R, Perry G, Morin B. Improvements in blast fragmentation models using digital image processing. In: *Proceedings of the 38th rock mechanics symposium*. Washington; 2001.
- [21] Esen S, Bilgin HA. Effect of explosive on fragmentation. In: *Proceeding the 7th international conference on mining, petroleum and metallurgical engineering*. Assiut; 2001.